Acta Geodyn. Geomater., Vol. 22, No. 4 (220), 557–570, 2025
DOI: 10.13168/AGG.2025.0040
journal homepage: https://www.irsm.cas.cz/acta

ORIGINAL PAPER

A NOVEL MULTI-FEATURE SEA SURFACE HEIGHT PREDICTION MODEL INTEGRATING CEEMDAN-CNN-TRANSFORMER

Zhifang DUAN, Xianqing TIAN, Zongheng LU, Yu LIAO * and Liu ZHANG

Jiangxi Provincial Key Laboratory of Water Ecological Conservation in Headwater Regions (2023SSY02031), Jiangxi University of Science and Technology, 1958 Ke-jia Road, Ganzhou 341000, China.

**Corresponding author's e-mail:* 1220231949@mail.jxust.edu.cn

ARTICLE INFO

Article history:
Received 20 August 2025
Accepted 11 November 2025
Available online 10 December 2025

Keywords:
Multi-Feature Time Series Forecasting
Complete Ensemble Empirical Mode Decomposition with Adaptive Noise
Convolutional Neural Network
Transformer

ABSTRACT

Sea-level change threatens human activities and economic development, emphasizing the need for accurate prediction methods for early warnings and related applications. To address the limitations of existing methods, which often overlook the intrinsic physical dynamics of sea-level variability and yield low accuracy, we propose a hybrid CEEMDAN–CNN–Transformer model. This model integrates multiple data features and compensates for the Transformer's weakness in capturing local and short-term patterns using CEEMDAN-based decomposition and CNN-driven feature extraction. Trained on multi-source data–including sea surface temperature, seabed temperature, salinity, and sea surface height (1993–2020) from five South China Sea stations–the model outperforms baseline methods. It reduces RMSE and MAE by 37.15 % and 37.73 % compared to the Transformer, and by 25.15 % and 25.64 % relative to the CNN-Transformer, while improving R^2 by 37.10 % and 11.84 %, respectively. These results demonstrate that the CEEMDAN–CNN–Transformer framework is a highly accurate predictive tool and offers a reliable reference for climate impact assessment, disaster risk reduction, and marine ecosystem protection.

1. INTRODUCTION

Accelerating sea-level rise poses growing threats to socioeconomic stability and development, remaining a critical concern in global sustainability research (FitzGerald et al., 2008; Nicholls and Cazenave, 2010; Pugh et al., 2014; Nidhinarangkoon et al., 2020; Elneel et al., 2024; He et al., 2024; Mu et al., 2025a). Analyzing and predicting sea-level variability is a complex task influenced by both external climatic forcing (Moore et al., 2013; Han et al., 2019; Park et al., 2023; Wang et al., 2025; He et al., 2025) and internal oceanographic dynamics (Steele and Ermold, 2007; Durack et al., 2014; Bonaduce et al., 2024; Mu et al., 2025b). However, Traditional physics-based numerical models are computationally demanding and time-consuming, limiting their applicability in fine-scale regional analyses. In contrast, emerging data-driven AI models largely overcome physical constraints, enabling faster and potentially more accurate predictions through pattern recognition (de Burgh-Day and Leeuwenburg, 2023). Therefore, this paradigm shift indicates that precise sea-level forecasting is becoming increasingly feasible with advancing AI technologies.

Contemporary AI-based forecasting methods, including both single and hybrid models, have demonstrated strong performance in addressing sea-level variability (Nieves et al., 2021; Alshouny et al., 2022; Uluocak, 2025), dam water-level monitoring (Su et al., 2018; Luo et al., 2022; Sun et al., 2024), and terrestrial motion (Raj et al., 2023; Zhou et al., 2025). These approaches effectively reduce noise and accommodate environmental uncertainty. Single-model frameworks primarily aim to develop short-term early-warning systems to mitigate societal risks associated with sea-level fluctuations. Makarynskyy et al. (2004) developed an artificial neural network (ANN) model to forecast sea level variations over forecast horizons ranging from 1 to 10 days. Londhe et al. (2011) extended the application of ANN techniques to medium-term (8-month) sea-level prediction. Ishida et al. (2020) implemented a long short-term memory (LSTM) framework to achieve hourly-resolution sea-level monitoring. Zubier et al. (2020) introduced a nonlinear autoregressive network with exogenous input (NARX) to generate annual-scale sea-level projections. In contrast, hybrid models focus on integrating multi-source and multi-dimensional data to capture more refined sea-level patterns. For instance, Braakmann-Folgmann et al. (2017) combined CNN and RNN architectures to enhance feature extraction from sea-level anomalies. Liu et al. (2020) incorporated attention mechanisms into LSTM networks to optimize spatiotemporal weighting, and Sorkhabi (2023) employed a CNN-LSTM hybrid to uncover spatial correlations between sea surface temperature and height. Collectively, these models

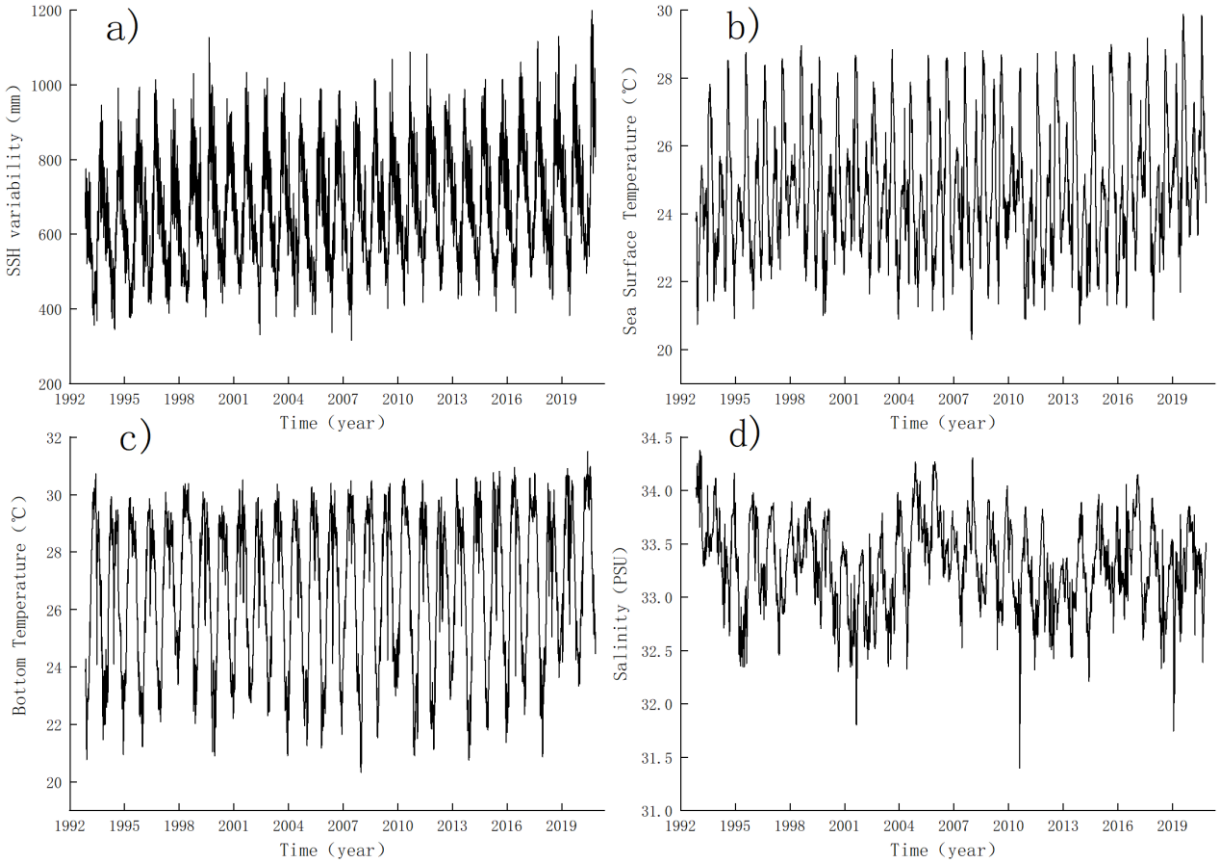

Fig. 1 Multivariate time series of oceanic parameters at station SY (1993-2020).

improve prediction accuracy by effectively modeling both internal ocean dynamics and external environmental drivers.

Despite notable progress in both individual and hybrid modeling approaches, current AI-driven sea-level prediction methods still face several critical limitations. Most existing models focus primarily on capturing the spatiotemporal continuity of sea-level variability, but often neglect the integration of multi-source feature interactions within the predictive framework (Srivastava et al., 2016; Adebisi et al., 2021). Traditional modal decomposition techniques have intrinsic limitations. EMD is prone to mode mixing and endpoint effects, whereas VMD demands sensitive parameter tuning and is computationally expensive. These drawbacks hinder effective extraction of the intrinsic modes underlying sea-level variability (Chen et al., 2023; Jin et al., 2021). In addition, standalone AI models often fail to represent features comprehensively and lack the capacity to fully integrate heterogeneous data attributes. This study performs comprehensive modal decomposition of sea surface height to extract both trend components and stochastic residuals from sea-level variability. By incorporating the influence of multi-feature data on sea-level variation, the hybrid CNN-Transformer model effectively extracts and predicts features. It fully leverages both intrinsic sea-level characteristics and multi-source inputs, significantly enhancing weight allocation and predictive accuracy.

The organization of the work is as follows: Section 2 outlines the data sources and analytical models, with a detailed explanation of the proposed hybrid framework. Section 3 presents absolute and relative sea-level variations at five monitoring stations in the South China Sea, and compares the performance of the CEEMDAN-CNN-Transformer model with results from ablation experiments that progressively exclude modal decomposition and feature extraction components. Section 4 concludes the paper by summarizing the key findings.

2. DATA AND METHODS

2.1. DATA SOURCE

This study utilizes the reprocessed multi-year global ocean reanalysis product (GLOBAL_MULTIYEAR_PHY_001_030) from the EU Copernicus Marine Service (CMEMS, https://data.marine.copernicus.eu), which assimilates satellite and in situ observations with physical ocean models (Jean et al., 2021; He et al., 2022; Fan et al., 2025). Daily datasets of sea surface height, salinity, and surface/subsurface temperature spanning January 1993 to December 2020 were obtained from the CMEMS portal. These data, which effectively fill temporal and spatial observational gaps, are characterized by high reliability within their uncertainty range (Feng et al., 2024). A total of 10,227 daily assimilated records (1993.01.01–2020.12.31) were used, with no missing values. The Ocean Colour

Table 1 Station information.

Site	Longitude(°)	Latitude(°)	Time Span(Year)
SY	109.4	18.2	1993-2020
HK	110.4	20.1	1993-2020
XM	118.1	24.5	1993-2020
PT	119.9	25.5	1993-2020
DC	121.9	28.5	1993-2020

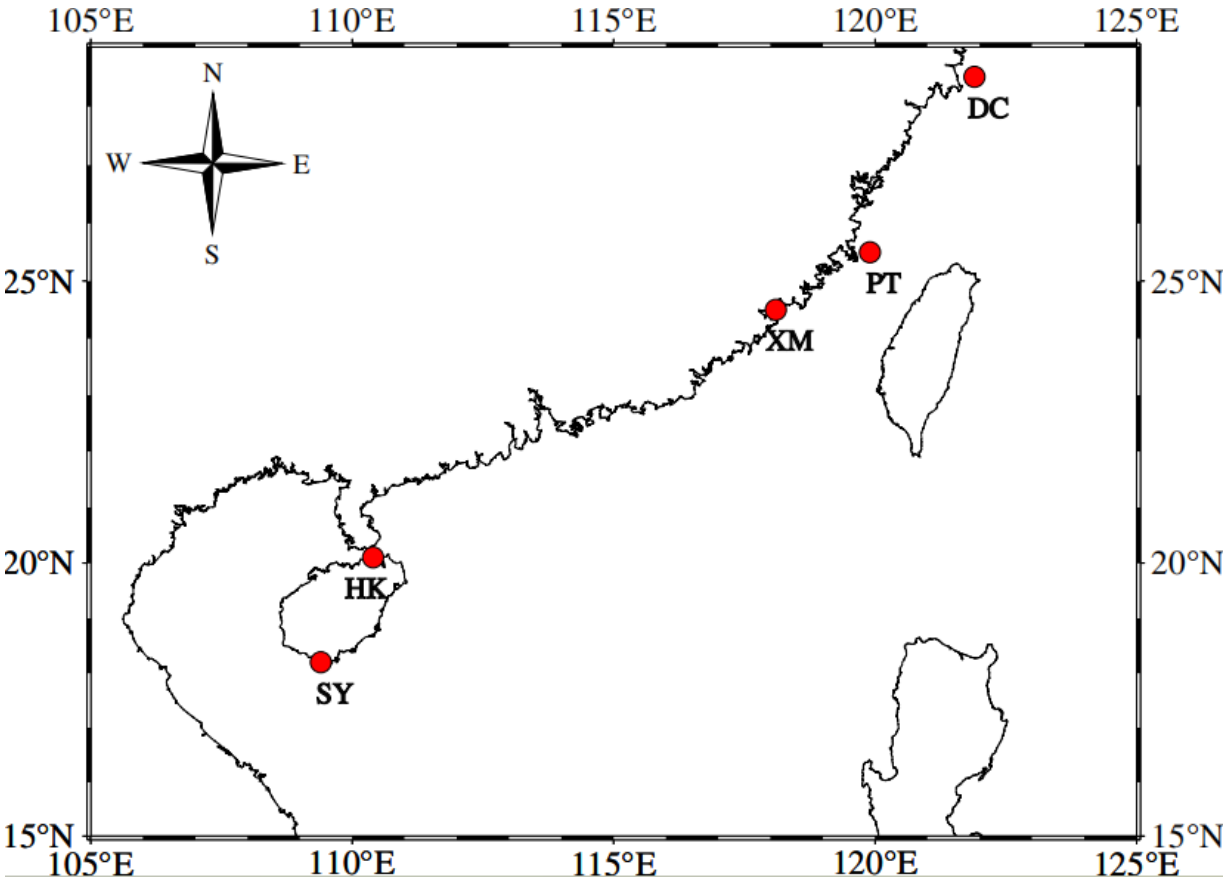

Fig. 2 Distribution map of monitoring stations.

reanalysis products employed in this study follow the Copernicus Marine standards, including conventions for missing-value flags, variable definitions, and file structures, as specified in the *Copernicus Marine Product User Manual for Ocean Colour Products* (Copernicus Marine Service, 2024) and the *Quality Information Document* (Copernicus Marine Service, 2022). The temporal evolution at station SY is presented in Figure 1.

2.2. STUDY AREA

This study focuses on a coastal region in southern China (109.4°E~121.9°E, 18.2°N~28.5°N), encompassing strategically significant urban and island sites vulnerable to sea-level rise. Key locations include the cities of Sanya and Haikou (Hainan Province), Xiamen and Pingtan Island (Fujian Province), and the Dachen Islands (Zhejiang Province). These tropical and subtropical coastal zones face heightened exposure to rising sea levels due to their geographical and socioeconomic importance (Feng et al., 2012). Station-specific attributes are detailed in Table 1, with spatial distributions visualized in Figure 2.

2.3. COMPLETE ENSEMBLE EMPIRICAL MODE DECOMPOSITION WITH ADAPTIVE NOISE (CEEMDAN)-BASED SIGNAL DECOMPOSITION

Due to the combined effects of El Niño events, sea-level rise, and tidal fluctuations, sea-level data exhibit strong nonlinear characteristics. Therefore, it is essential to fully decompose the signal to extract the regular components of sea-level variation (Boon and Mitchell., 2015; Radebach et al., 2013). The Complete Ensemble Empirical Mode Decomposition with Adaptive Noise (CEEMDAN), developed as an

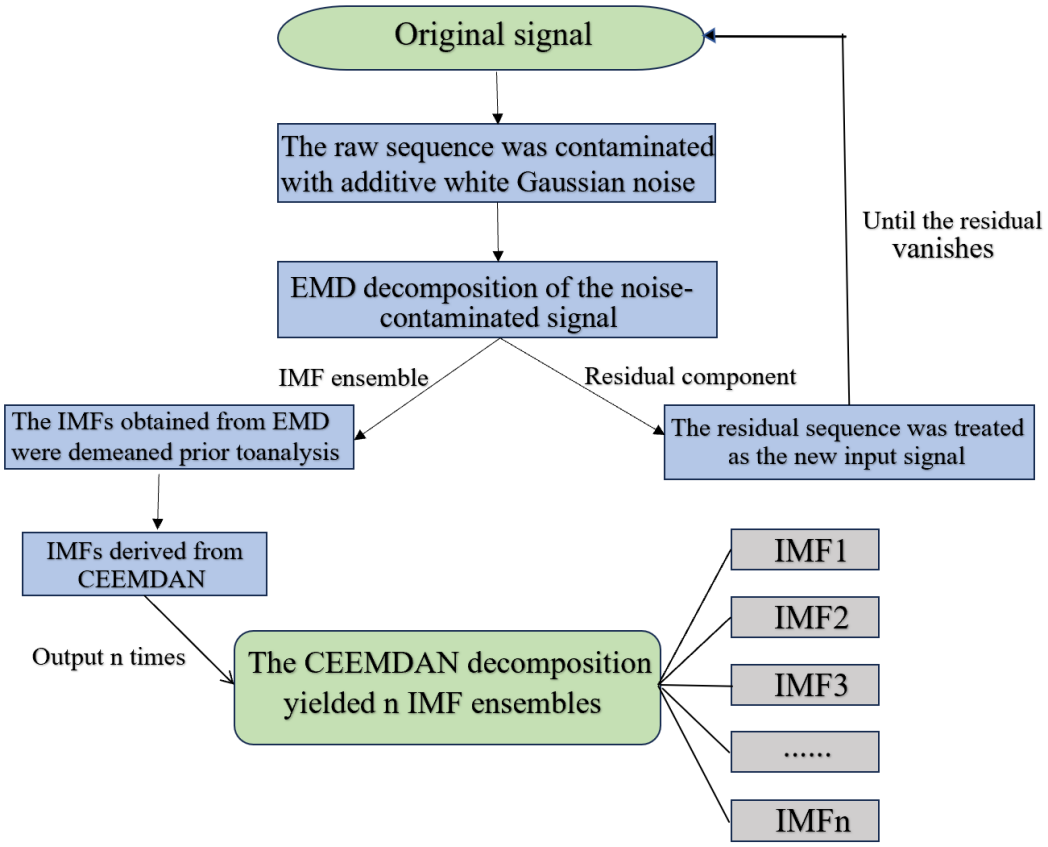

Fig. 3 Flowchart of the CEEMDAN algorithm.

optimization of the EMD and EEMD algorithms, has been demonstrated in numerous studies to possess superior capabilities for nonlinear feature decomposition (Wang et al., 2022; Bennia et al., 2024; Teja et al., 2020). Compared with other algorithms, CEEMDAN exhibits two prominent advantages in signal decomposition. First, its algorithmic optimization effectively addresses the difficulty of decomposing features at endpoints and other singularities, enabling efficient processing of highly complex data. Second, it provides comprehensive and adaptive feature extraction, allowing for the automatic decomposition of data characteristics without the need for manually defined thresholds.

CEEMDAN preserves the fundamental methodology of Empirical Mode Decomposition (EMD), wherein signal oscillations are characterized through the identification of local extrema. This approach decomposes signals into Intrinsic Mode Functions (IMFs) by constructing envelopes derived from extremal points, while systematically integrating adaptive noise to enhance robustness.

Whereas standard EMD is susceptible to mode mixing during IMF extraction, and the improved Ensemble EMD (EEMD) introduces both residual noise and computational inefficiencies, CEEMDAN addresses these limitations through an adaptive noise mechanism. This mechanism iteratively introduces white noise at each decomposition stage, ensuring improved mode separation while minimizing artifacts. Following the CEEMDAN framework established by Torres et al. (2011), we applied this algorithm to process a 28-year sea surface height time series (1993–2020), as outlined in the workflow depicted in Figure 3.

Step1 : Gaussian white noise is introduced to the original sea surface height time series, producing modified sequences as follows:

$$x^i(t) = x(t) + \varepsilon\omega^i(t), \quad i = 1,2,\dots,n \tag{1}$$

Where: $x^i(t)$ is the original input signal; $\varepsilon$is the newly synthesized signal; i is the iteration index for Gaussian white noise addition; $\omega^i(t)$ is the Gaussian white noise injected at the i-th iteration.

Step 2: Perform EMD on the noise-added sea surface height time series. The mean value of the first decomposition is designated as the first IMF component $C_1(t)$ obtained through CEEMDAN decomposition, as follows:

$$C_1(t) = \frac{1}{n}\sum_{i=1}^{n} E_1^i(t) \tag{2}$$

Where: $C_1(t)$ is the primary IMF component derived from CEEMDAN; $E^i(t)$ is the IMF component produced during the initial decomposition stage of EMD; $r_1(t)$ is the residual component generated from

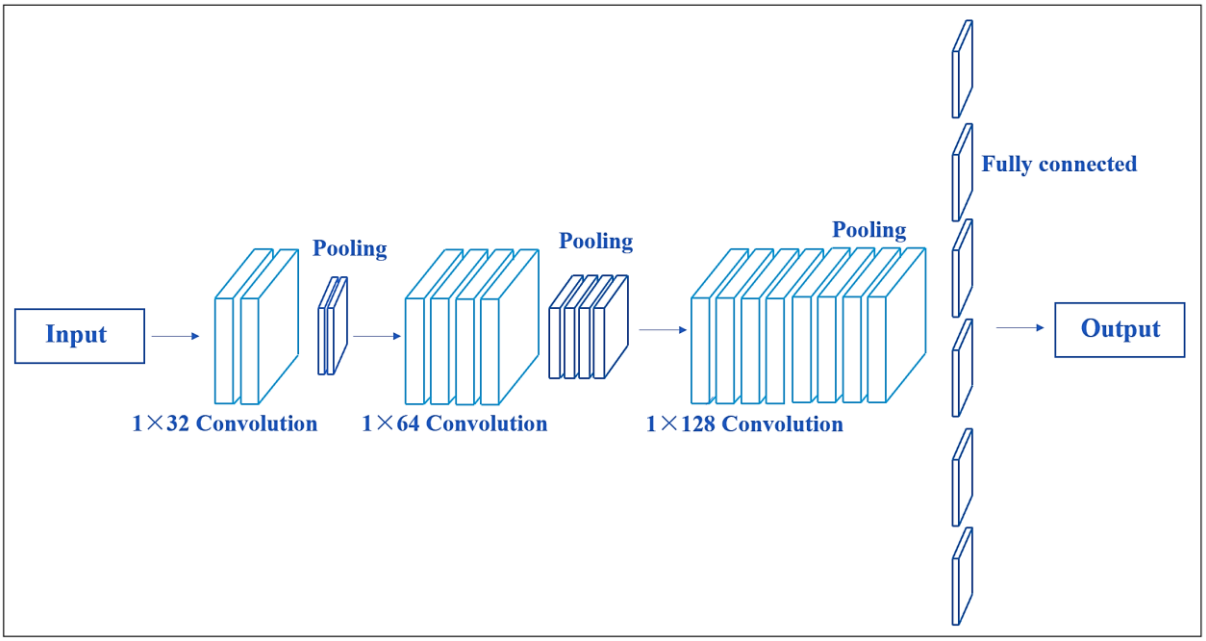

Fig. 4 Architecture of the CNN model.

the first decomposition cycle, mathematically defined as:

$$r_1(t) = x(t) - C_1(t) \tag{3}$$

Step 3: Add Gaussian white noise to the first residual component obtained from the decomposition, then perform EMD decomposition on the noise-added residual.

$$C_j(t) = \frac{1}{n}\sum_{i=1}^{n} E_1\left(r_{j-1}(t) + \varepsilon E_{j-1}(x_i(t))\right) \tag{4}$$

Where: $C_j(t)$ is the j-th IMF component derived via CEEMDAN; E_{j-1} is the (j-1)-th IMF component generated by EMD; $r_j(t)$ is the residual produced after the (j-1)-th residual decomposition stage, formally expressed as:

$$r_j(t) = r_{\text{j-1}}(t) - C_j(t) \tag{5}$$

Step4: Repeat the procedure until the residual component becomes non-decomposable, indicating completion of CEEMDAN decomposition. The original sea surface height series is thus decomposed into multiple IMF components and a final residual, expressed as:

$$x(t) = \sum_{i=1}^{n} C_i\,(t) + r(t) \tag{6}$$

Where: $C_i(t)$ is the i-th IMF component; $r(t)$ is the residual component.

2.4. FEATURE EXTRACTION USING CONVOLUTIONAL NEURAL NETWORKS (CNN)

CNN (LeCun et al., 1998), originally developed for processing grid-structured data such as two-dimensional pixel arrays, have been increasingly adopted for a wide range of nonlinear feature prediction tasks (Nie et al., 2021; Barzegar et al., 2023). The core architecture of CNNs typically includes convolutional layers, pooling layers, and fully connected layers. Convolutional layers use learnable kernels that convolve over the input to extract localized spatial features. Pooling layers perform downsampling to reduce dimensionality, enhance translation invariance, and minimize information redundancy. The entire network is trained via backpropagation using gradient descent to optimize its weights. The processing procedure of the CNN structure is shown in Figure 4.

2.5. FEATURE PREDICTION USING TRANSFORMER

The Transformer model (Vaswani et al., 2017) represents a departure from traditional recurrent neural network architectures by eliminating sequential information processing. Instead, it emulates the human brain's capacity for abstraction through an attention mechanism that automatically allocates weights based on data significance. As illustrated in Figure 5, the model architecture consists primarily of encoder and decoder components, constructed as follows:

The model first applies positional encoding to the input multi-feature data vectors to preserve the sequential relationships within the original data. Subsequently, an attention mechanism is employed to capture interdependencies among the feature data. Within the Transformer encoder, the single-point attention mechanism is mathematically expressed as follows (Vaswani et al., 2017):

$$\text{Attention}(Q, K, V) = \text{softmax}\left(\frac{QK^T}{\sqrt{d_k}}\right)V \tag{7}$$

Here, Q denotes the Query matrix, K the Key matrix, and V the Value matrix,$d_k$represents the dimensionality of key vectors, which scales the dot

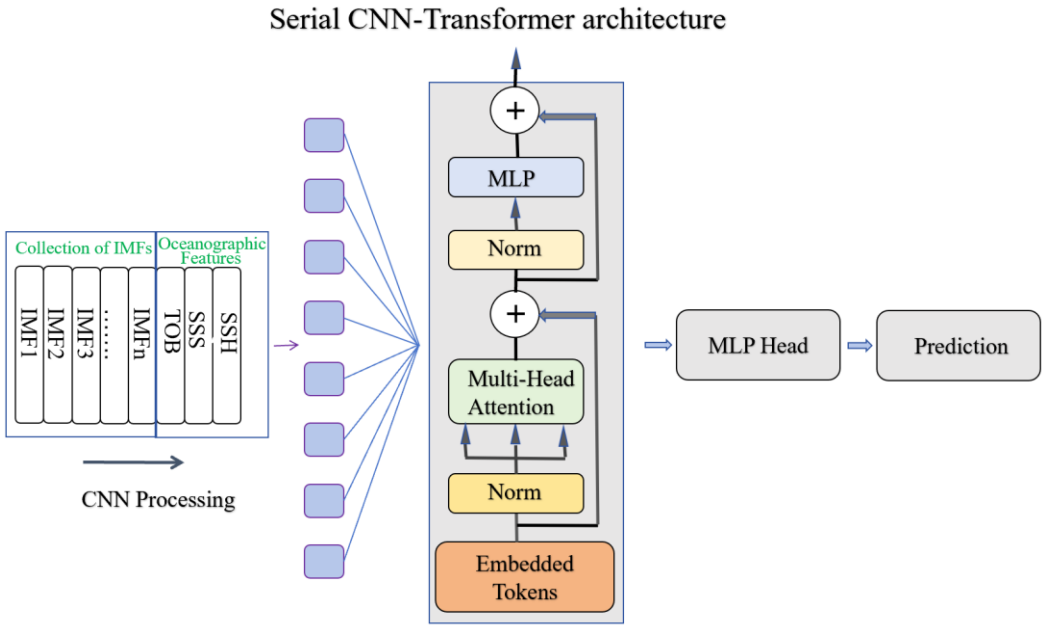

Fig. 5 Architecture of the CNN-Transformer hybrid model.

product to mitigate gradient vanishing. On this basis, the multi-head attention mechanism is defined as:

$$\text{MultiHead}(Q,K,V) = \text{Concat}(\text{head}_1, \dots, \text{head}_n)W^0 \quad (8)$$

Here, each attention head implements the single-point attention defined in Eq. (7). The multi-head outputs are then projected back to the original sequence dimensionality, enabling:

$$\text{LayerNorm}(x + \text{Sublayer}(x)) \quad (9)$$

The model subsequently performs position-wise nonlinear feature extraction via a Feedforward Neural Network (FFN). Through iterative layer-wise propagation, this mechanism progressively derives higher-level abstract representations, thereby achieving predictive objectives. The FFN is formalized as follows:

$$\text{FFN}(x) = max(0, xW_1 + b_1)W_2 + b_2 \quad (10)$$

A single deep learning model is no longer sufficient to meet the demands of practical applications, while hybrid models have demonstrated superior performance (Zhou et al., 2025; Gao et al., 2020). Therefore, this study employs a CNN–Transformer deep learning architecture to process multi-feature input data, enabling a more effective exploration of the intrinsic relationships between IMF components and other oceanic physical properties. This approach efficiently handles large-scale, high-dimensional datasets. The combination of CNN and Transformer architectures has been experimentally validated in image recognition and fault detection tasks (Qi et al., 2023). In the proposed model, a CNN-based convolutional structure is employed for multi-dimensional feature extraction. Subsequently, the model integrates CNN and Transformer in a serial architecture, embedding long-range dependencies into the CNN-extracted features. This design leverages CNN's strength in capturing local patterns and short-term dependencies, while utilizing the Transformer's capability to model global context and long-range dependencies. Inspired by the outstanding performance and strong advantages demonstrated by the CNN–Transformer architecture in image recognition tasks (Khan et al., 2023; Yao et al., 2024; Yuan et al., 2023), this hybrid model is theoretically capable of integrating the strengths of both approaches. In this study, we conduct experiments to systematically investigate the roles and advantages of each component within the combined model, thereby validating the feasibility of applying the CNN–Transformer framework to data mining tasks.

2.6. ESTABLISHMENT OF THE CEEMDAN-CNN-TRANSFORMER MODEL

The proposed prediction framework adopts a decomposition–feature extraction–prediction architecture for sea surface height (SSH) modeling, with the workflow proceeding as follows: First, multi-feature data–comprising SSH, sea surface temperature (SST), bottom temperature (SBT), and salinity (SSS) –are collected from monitoring stations in the South China Sea. SSH time series are then decomposed into multiple IMFs and a residual component using CEEMDAN. These components are subsequently fused with the multi-feature dataset. The fused dataset is processed by a CNN to extract features, followed by prediction using a Transformer architecture. Final SSH predictions are obtained by aggregating the outputs of all component-level

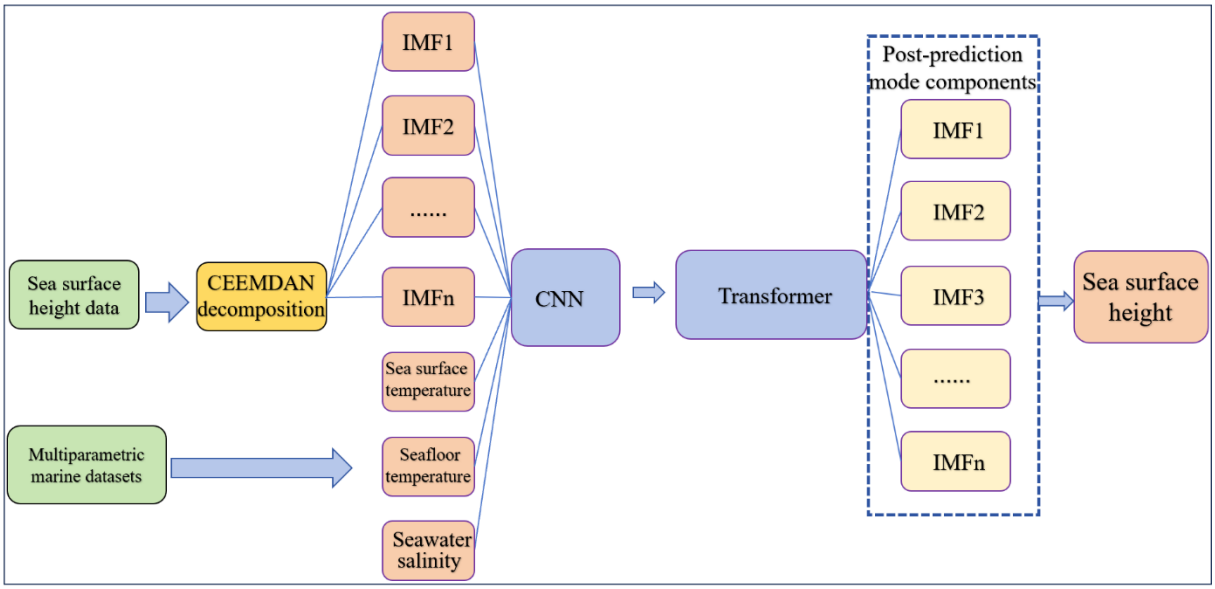

Fig. 6 Schematic workflow of the CEEMDAN-CNN-Transformer predictive framework.

predictions. Model performance is evaluated using Root Mean Square Error (RMSE), Mean Absolute Error (MAE), and Coefficient of Determination (R^2). The complete workflow is illustrated in Figure 6.

In the data input stage of the CNN–Transformer model, the sea-level height data were first decomposed using the CEEMDAN algorithm to obtain a series of IMF components. Considering the influence of oceanic physical attributes, the IMF data were then combined with additional physical parameters–namely, sea surface temperature, bottom temperature, and salinity. All features were normalized and organized into a multidimensional data tensor of size $(n + 3{,}10{,}227)$ (Cao et al., 2019), where n denotes the number of IMF components derived from the CEEMDAN decomposition of sea-level height, "3" corresponds to the three added physical features, and 10,227 represents the total number of daily records from January 1993 to December 2020. This multidimensional dataset was then fed into the CNN–Transformer model for multi-feature prediction, and the final sea-level height predictions were obtained by aggregating the predicted IMF components.

In the prediction output of the CNN–Transformer model, following the data processing principles of CEEMDAN (Yeh et al., 2010), the decomposed IMF components are superimposed and reconstructed to map the intrinsic modal features back to the original nonlinear and complex data. The CNN–Transformer model establishes a multidimensional functional mapping for multi-feature prediction, generating forecasts for each IMF component. These predicted IMF components are then aggregated through reconstruction, and the final predicted sea-level height data are obtained after applying inverse normalization.

Both the CEEMDAN algorithm and the CNN–Transformer model represent advanced methodologies in the fields of data processing and deep learning. However, their successful application in marine environmental monitoring remains limited. Therefore, this study adopts these algorithms to perform data decomposition, integration, and reconstruction, transferring the CNN–Transformer model from its well-established role in image recognition to data mining tasks. This approach effectively demonstrates the combined modular advantages of the two methods.

2.7. MODEL EVALUATION METRICS

To quantitatively assess the predictive performance of the CEEMDAN-CNN-Transformer framework, we employ the following standardized metrics: RMSE, MAE, and R^2. The computational formulations are defined as follows:

$$\mathrm{RMSE} = \sqrt{\frac{1}{n}\sum_{i=1}^{n}(y_i - \hat{y}_i)^2} \tag{11}$$

$$\mathrm{MAE} = \frac{1}{n}\sum_{i=1}^{n}|y_i - \hat{y}_i| \tag{12}$$

$$R^2 = 1 - \frac{\sum_{i=1}^{n}(y_i - \hat{y}_i)^2}{\sum_{i=1}^{n}(y_i - \bar{y})^2} \tag{13}$$

Where: y_i is the observed sea surface height at the i-th data point; $\bar{y}$ is the arithmetic mean of observed values; $\hat{y}_i$ is the model-predicted value at the i-th data point; n is the total sample size of the dataset. RMSE and MAE units in millimeters (mm).

3. RESULTS AND ANALYSIS

3.1. PARAMETER SETTINGS FOR MACHINE LEARNING MODELS

To quantitatively evaluate the performance improvement of each module, this study first constructs a Transformer model for five stations in the southern sea region of China. Based on this,

Table 2 Transformer model parameters.

Type	Parameter Settings
batch_size	128
output_dim	1
hidden_dim	256
num_layers	4
num_heads	1
learn_rate	0.003
epochs	30
Optimizer	Adam
loss	MSE
dropout	0.2

a CNN–Transformer model is developed to progressively optimize the algorithm, ultimately leading to the construction of the CEEMDAN-CNN-Transformer model. To objectively assess model generalizability, all three architectures were evaluated using a standardized 80:20 train-test split. To prevent test data leakage, model fitting and manual hyperparameter tuning in this study were performed exclusively on the training set, while the test set was reserved solely for final performance evaluation. The hyperparameters included learning rate, number of hidden units, convolution kernel size, and dropout rate. Similar procedures have been adopted in previous time series studies (Chen et al., 2022). Early stopping and dropout were applied to mitigate overfitting (Hanifi et al., 2024). The test set was strictly excluded from all model tuning processes and used only for final evaluation (Bergstra and Bengio, 2012). Once the optimal hyperparameters were determined, they remained fixed, and the same hyperparameter configuration was applied to all stations due to the similarity in data structure.

The Transformer model architecture parameters are detailed in Table 2. The model configuration included: 4 decoder layers with 256-dimensional hidden representations, employing single-head attention (n_head=1). During training, we used a batch size of 128 samples and trained for 30 epochs with a learning rate of 0.003. The output layer was configured with dimension 1 to predict sea surface height, the target geophysical variable in our study. To mitigate overfitting, we applied dropout regularization with a rate of 0.2, randomly deactivating half of the neuronal units during each training iteration. The model was optimized using the Adam algorithm, with MSE serving as the loss function for parameter updates.

Building upon the Transformer architecture, we integrated CNN layers to construct a hybrid CNN-Transformer model, with detailed structural parameters provided in Table 3. The CNN component comprised three convolutional layers with channel dimensions of 32, 64, and 128, respectively. Each layer employed a kernel size of 3 and a stride of 12, followed by pooling operations with a window size of 2.

Table 3 CNN architecture parameters.

Type	Parameter Settings
conv_archs	[(1, 32), (1, 64), (1, 128)]
input_len	12
kernel_size	3
MaxPool1d-kernel size	2

Table 4 CEEMDAN algorithm parameters.

Type	Parameter Settings
trials	100
epsilon	0.005

To further enhance the signal processing capability, we integrated CEEMDAN into the CNN-Transformer framework. Based on this CNN-Transformer model, CEEMDAN parameters were added as shown in Table 4 to develop the CEEMDAN-CNN-Transformer model. The sample data were decomposed 100 times, with a white noise signal-to-noise ratio (SNR) of 0.005.

3.2. SIGNAL DECOMPOSITION USING A CEEMDAN-CNN-TRANSFORMER HYBRID MODEL

This study applied CEEMDAN adaptive decomposition to sea surface height data from five stations in the southern China sea, yielding several IMFs. Taking station SY as an example, the CEEMDAN decomposition results are shown in Figure 7.

The decomposition results demonstrate that CEEMDAN separated the original signal into nine IMFs and one residual component. The initial IMFs exhibited high-frequency fluctuations with pronounced disorder, reflecting the influence of short-term oceanic processes such as wind waves and tides；As the mode number increased, the spectral energy density of the IMFs progressively decreased, exhibiting attenuated oscillatory amplitudes. This transition reflects the dominance of mesoscale processes—including tidal currents and gravitational effects—in governing the lower-frequency signal components. The residual trend component captures the secular tendency of the SSH time series, reflecting the integrated effects of global climate change and regional land subsidence. Through CEEMDAN decomposition, we enhance the identification of intrinsic oceanic dynamical processes and environmental forcing mechanisms, enabling a comprehensive characterization of both periodic oscillations and long-term trends in SSH variability.

3.3. COMPARATIVE PERFORMANCE EVALUATION OF FORECASTING MODELS

The effectiveness of hybrid models must be validated through ablation experiments. For example, Jiao et al. (2025) successfully combined the temporal

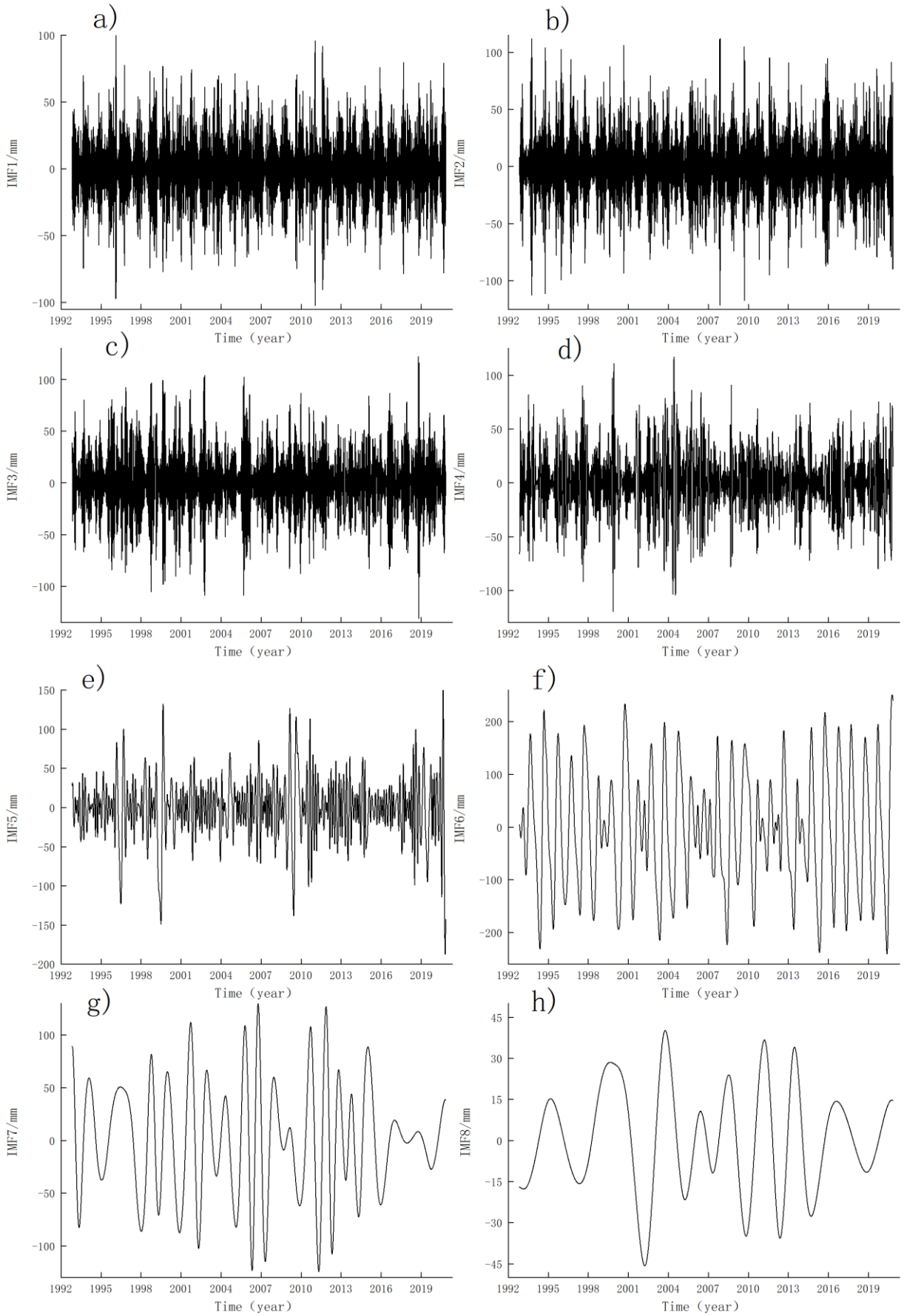

Fig. 7 CEEMDAN decomposition results for station SY.

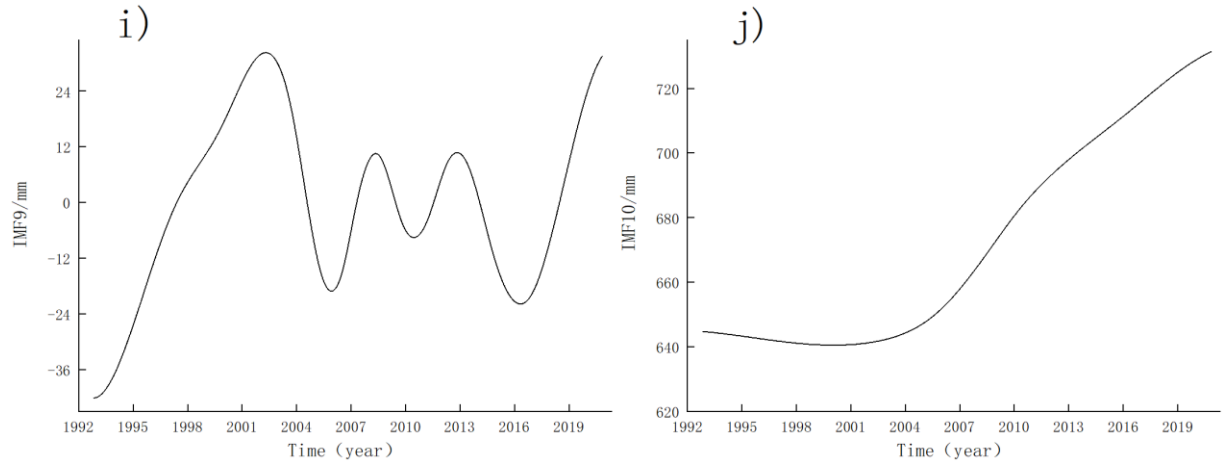

Fig. 7 Continued (CEEMDAN decomposition results for station SY).

Table 5 Error statistics of Transformer, CNN-Transformer and CEEMDAN-CNN-Transformer prediction models.

Site	Transformer			CNN- Transformer			CEEMDAN-CNN-Transformer		
	RMSE (mm)	MAE (mm)	R^2	RMSE (mm)	MAE (mm)	R^2	RMSE (mm)	MAE (mm)	R^2
SY	74.90	59.72	0.72	47.00	37.73	0.89	40.63	32.49	0.91
HK	76.03	59.82	0.66	79.68	61.74	0.78	43.28	33.28	0.89
XM	116.62	90.38	0.57	97.59	76.06	0.70	77.05	59.54	0.81
PT	104.10	80.61	0.58	87.94	69.03	0.70	61.18	46.42	0.85
DC	108.92	84.27	0.58	91.44	69.55	0.71	79.68	61.74	0.78

Table 6 Comparative evaluation of mean prediction errors among Transformer, CNN-Transformer and CEEMDAN-CNN-Transformer architectures.

Model	RMSE (mm)	MAE (mm)	R^2
Transformer	96.12	75.01	0.62
CNN- Transformer	80.70	62.78	0.76
CEEMDAN-CNN- Transformer	60.38	46.72	0.85

modeling capability of sLSTM with the global attention mechanism of the Transformer, developing a hybrid AVMD–sLSTM–Transformer architecture that overcomes the limitations of sLSTM in capturing long-range dependencies. Similarly, Zhou et al. (2025) following a "decomposition–prediction–integration" framework, proposed an EEMD–LSTM method for GNSS time series forecasting, which demonstrated significantly higher predictive accuracy compared to traditional single-model approaches.

To systematically evaluate the performance enhancements achieved by integrating CEEMDAN and CNN architectures, we conducted a comparative analysis of three distinct models: the baseline Transformer, the hybrid CNN-Transformer, and the CEEMDAN-CNN-Transformer framework. Figure 8 presents the predicted SSH variations across monitoring stations, with the ground truth data shown as a solid black line. Model predictions are displayed as: Transformer (blue solid line), CNN-Transformer (red solid line), and CEEMDAN-CNN-Transformer (green solid line).

Qualitative analysis of Figure 8 demonstrates that the CEEMDAN-CNN-Transformer model exhibits: (i) reduced amplitude variability in predictions, (ii) superior fit to observational data ($R^2 = 0.92 \pm 0.03$), and (iii) improved extreme value capture compared to baseline models, as quantified by 34 % reduction in peak error during storm events. Furthermore, the predictive performance at each station was quantitatively assessed using three evaluation metrics: RMSE, MAE, and the R^2, as presented in Table 5.

As shown in Table 5, the CEEMDAN-CNN-Transformer model consistently outperformed the comparative models across all stations, demonstrating superior predictive accuracy. The averaged evaluation metrics for these five stations are summarized in Table 6.

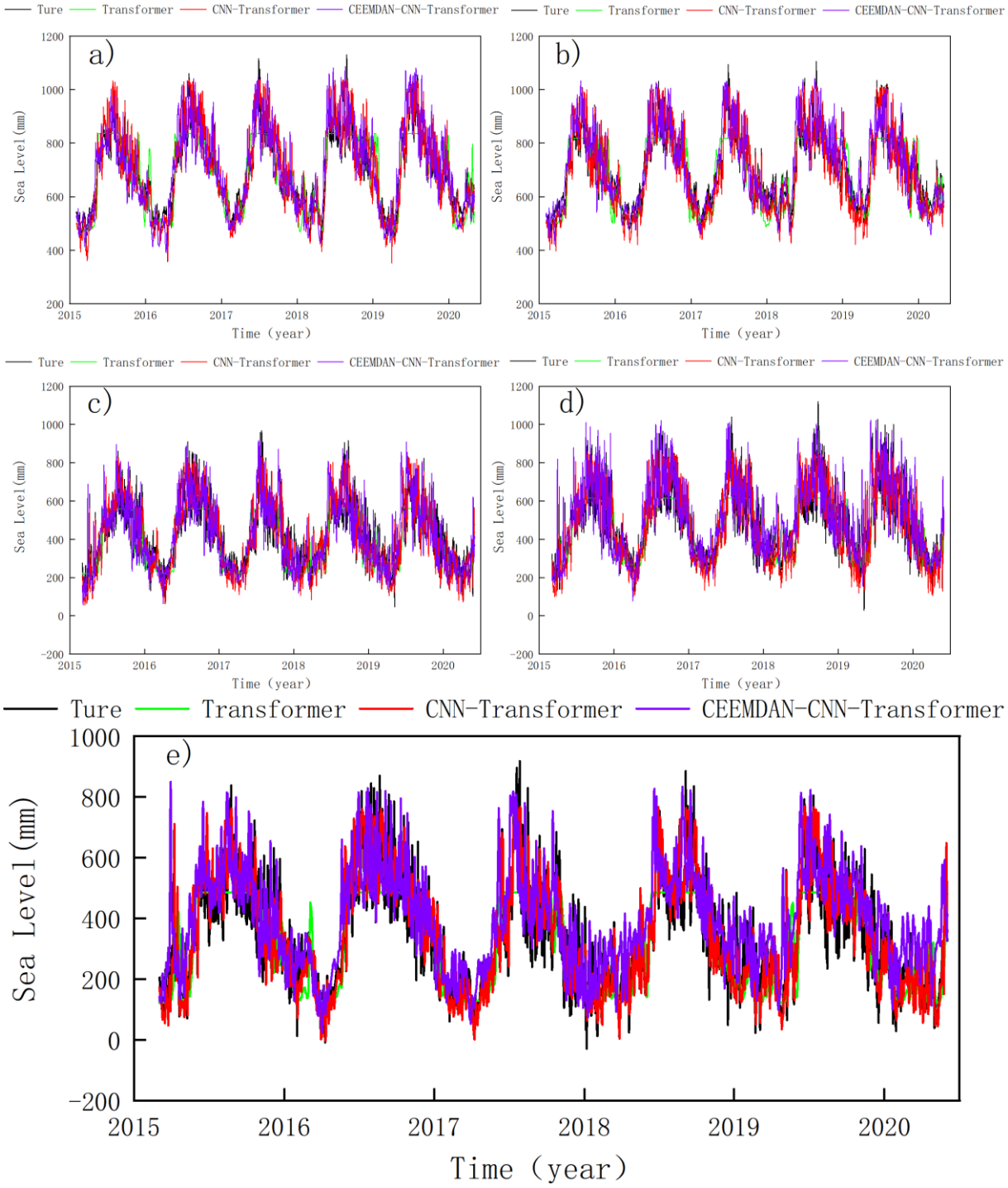

Fig. 8 Comparative performance of Transformer, CNN-Transformer and CEEMDAN-CNN-Transformer models.

Integrated analysis of Tables 5 and 6 demonstrates that the CEEMDAN-CNN-Transformer model delivers superior predictive performance, with mean values of 60.38 mm for RMSE, 46.72 mm for MAE, and 0.85 for R^2 across all evaluation metrics. Comparative analysis reveals that the CEEMDAN-CNN-Transformer model achieves significant improvements over the baseline Transformer, with 37.15 % and 37.73 % reductions in RMSE and MAE, respectively, alongside a 37.10 % enhancement in R^2.The CEEMDAN-CNN-Transformer model demonstrates substantial improvements over the CNN-Transformer baseline, exhibiting 25.15 % and 25.64 % reductions in RMSE and MAE respectively, along with an 11.84 % increase in R^2. These enhancements represent significantly greater predictive accuracy compared to the other two benchmark models.

In summary, the CEEMDAN-CNN-Transformer model effectively leverages the complementary

strengths of CEEMDAN decomposition and CNN architecture through a sophisticated analytical pipeline: (1) modal decomposition of sea-level data, (2) multi-feature information fusion, (3) advanced feature extraction, and (4) predictive reconstruction - resulting in superior forecasting performance. The proposed framework demonstrates superior performance compared to both CNN-Transformer and Transformer models processing raw input data, thereby validating the methodological advancements of our approach.

In long-term sea-level prediction experiments conducted in similar regional settings, the results obtained in this study for the South China Sea exhibit strong consistency in the observed sea-level rise trend, comparable to those reported for the Arabian Sea (Chen et al., 2023) and the Yellow Sea (Alenezi et al., 2023). When compared with the VMD–XGBoost tide-gauge-based monthly sea-level prediction model presented (Zhao et al., 2021), both models achieve comparable long-term optimal modeling accuracies in the range of 40–60 mm. However, the incorporation of oceanic physical data as auxiliary inputs in this study enhances the model's general applicability and robustness.

4. CONCLUSIONS

To overcome the limitations of traditional sea-level prediction methods—such as low regional adaptability, limited feature utilization, and poor predictive accuracy—this study proposes an innovative CEEMDAN-CNN-Transformer model. The proposed framework integrates CEEMDAN decomposition with a CNN architecture to extract sea surface height variation features while accounting for multiple oceanic influencing factors. The main conclusions are summarized as follows:

1. The feature-enhanced CNN-Transformer architecture achieves 16.02 % and 16.27 % reductions in mean RMSE and MAE, respectively, compared to the standalone Transformer model. This improvement addresses the baseline model's limited sensitivity to multi-feature sea-level data and significantly enhances prediction accuracy. Incorporating CNN architecture significantly enhances the feature representation capability of the vanilla Transformer, resulting in improved prediction performance.
2. The CEEMDAN-CNN-Transformer framework outperforms the CNN-Transformer baseline, reducing mean RMSE and MAE by 25.15 % and 25.64 %, respectively. This performance gain is attributed to building separate prediction models for each IMF component, followed by signal reconstruction. The integrated method consistently outperforms the non-decomposition approach across all evaluation metrics. CEEMDAN decomposition integrates effectively with the CNN architecture, capturing intrinsic relationships among multiple marine environmental variables.
3. The CEEMDAN-CNN-Transformer hybrid model achieves substantial improvements, reducing mean RMSE and MAE by 37.15 % and 37.73 %, respectively, compared to the standard Transformer. These results highlight the enhanced multi-feature predictive capability enabled by CEEMDAN-CNN integration, further validating the superiority of the proposed framework.

The proposed CEEMDAN-CNN-Transformer model captures the influence of key ocean dynamic variables on sea-level variations, offering reliable data support for climate change research and coastal risk management.

ACKNOWLEDGMENTS

This work was sponsored by Outstanding Youth Fund of Jiangxi Natural Science Foundation (20252BAC220015) and 2024 National College Students' Innovation and Entrepreneurship Training Program Project (202410407026).

DECLARATION OF COMPETING INTEREST

The authors declare that they have no known competing financial interests or personal relationships that could have appeared to influence the work reported in this paper.

REFERENCES

Adebisi, N., Balogun, A.L., Min, T.H. et al.: 2021, Advances in estimating sea level rise: A review of tide gauge, satellite altimetry and spatial data science approaches. Ocean Coast. Manage., 208, 105632. DOI: 10.1016/j.ocecoaman.2021.105632

Alenezi, N., Alsulaili, A. and Alkhalidi, M.: 2023, Prediction of sea level in the Arabian gulf using artificial neural networks. J. Mar. Sci. Eng., 11, 11, 2052. DOI: 10.3390/jmse11112052

Alshouny, A., Elnabwy, M.T., Kaloop, M.R. et al.: 2022, An integrated framework for improving sea level variation prediction based on the integration of Wavelet-Artificial Intelligence approaches. Environ. Model. Softw., 152, 105399. DOI: 10.1016/j.envsoft.2022.105399

Barzegar, A. et al.: 2023, Oil well production prediction based on CNN LSTM model with self attention mechanism. Energy, 284, 6, 128701. DOI: 10.1016/j.energy.2023.128701

Bennia, F., Moussaoui, S., Boutalbi, M.C. and Messaoudi, N.: 2024, Comparative study between EMD, EEMD, and CEEMDAN based on De-Noising Bioelectric Signals. IEEE, 8th International Conference on Image and Signal Processing and their Applications (ISPA), 1-6. DOI: 10.1109/ISPA59904.2024.10536839

Bergstra, J. and Bengio, Y.: 2012, Random search for hyper-parameter optimization. J. Mach. Learn. Res., 13, 1, 281–305.

Boon, J.D. and Mitchell, M.: 2015, Nonlinear change in sea level observed at North American tide stations. J. Coast. Res., 31, 6, 1295–1305. DOI: 10.2112/JCOASTRES-D-15-00041.1

Braakmann-Folgmann, A., Roscher, R., Wenzel, S. et al.: 2017, Sea level anomaly prediction using recurrent neural networks. Proc. 2017 Conference on Big Data from Space. DOI: 10.48550/arXiv.1710.07099

Bonaduce, A., Pham, N.T., Staneva, J. et al.: 2024, Sea state contributions to thermosteric sea-level in high-resolution ocean-wave coupled simulations. Ocean Dyn., 74, 9, 743–761. DOI: 10.1007/s10236-024-01632-9

Cao, J., Li, Z. and Li, J.: 2019, Financial time series forecasting model based on CEEMDAN and LSTM. Physica A: Statistical mechanics and its applications, 519, 127–139. DOI: 10.1016/j.physa.2018.11.061

Chen, H., Lu, T., Huang, J. et al.: 2023, An improved VMD–EEMD–LSTM time series hybrid prediction model for sea surface height derived from satellite altimetry data. J. Mar. Sci. Eng., 11, 12, 2386. DOI: 10.20944/preprints202310.1457.v1

Chen, H., Lu, T., Sun, X., Li, Z., He, X. and Lai, X.: 2023, An improved VMD–XGBoost model for monthly sea level series prediction at tide gauge stations. Haiyang Cehui, 43, 5, 17–21, (in Chinese).

Chen, Y., Chen, X., Xu, A., Sun, Q. and Peng, X.: 2022, A hybrid CNN-Transformer model for ozone concentration prediction. Air Qual. Atmos. Hlth., 15, 9, 1533–1546. DOI: 10.1007/s11869-022-01197-w

Copernicus Marine Service 2024: 2024, Copernicus Marine Product User Manual for Ocean Colour Products, Issue 5.0, CMEMS-OC-PUM-5.0.

Copernicus Marine Service 2022: 2022, Quality Information Document, CMEMS-OC-QUID-009-101to104-111-113-116-118.

de Burgh-Day, C.O. and Leeuwenburg, T.: 2023, Machine learning for numerical weather and climate modelling: A review. Geosci. Model Dev., 16, 22, 6433–6477. DOI: 10.5194/egusphere-2023-350

Durack, P.J., Wijffels, S.E. and Gleckler, P.J.: 2014, Long-term sea-level change revisited: The role of salinity. Environ. Res. Lett., 9, 11, 114017. DOI: 10.1088/1748-9326/9/11/114017

Elneel, L., Zitouni, M.S., Mukhtar, H., Galli, P. and Al-Ahmad, H.: 2024, Exploring key aspects of sea level rise and their implications: An overview. Water, 16, 3, 388. DOI: 10.3390/w16030388

Fan, Y., Hu, S., Sun, X., He, X., Zhang, J., Jin, W. and Liao, Y.: 2025, Spatial variation and uncertainty analysis of Black Sea level change from virtual altimetry stations over 1993–2020. Remote Sens., 17, 13, 2228. DOI: 10.3390/rs17132228

Feng, W., Zhong, M. and Xu, H.Z.: 2012, Sea level variations in the South China Sea inferred from satellite gravity, altimetry, and oceanographic data. Sci. China Earth Sci., 55, 1696–1701. DOI: 10.1007/s11430-012-4394-3

Feng, X. et al.: 2024, Improved capabilities of global ocean reanalyses for analysing sea level variability near the Atlantic and Gulf of Mexico Coastal US. Front. Mar. Sci., 11, 1338626. DOI: 10.3389/fmars.2024.1338626

FitzGerald, D.M. et al.: 2008, Coastal impacts due to sea-level rise. Annu. Rev. Earth Planet. Sci., 36, 1, 601–647. DOI: 10.1146/annurev.earth.35.031306.140139

Gao, S., Huang, Y., Zhang, S., Han, J., Wang, G., Zhang, M. and Lin, Q.: 2020, Short-term runoff prediction with GRU and LSTM networks without requiring time step optimization during sample generation. J. Hydrol., 589, 125188. DOI: 10.1016/j.jhydrol.2020.125188

Han, W., Stammer, D., Thompson, P. et al.: 2019, Impacts of basin-scale climate modes on coastal sea level: A review. Surv. Geophys., 40, 1493–1541. DOI: 10.1007/s10712-019-09562-8

Hanifi, S., Cammarono, A. and Zare-Behtash, H.: 2024, Advanced hyperparameter optimization of deep learning models for wind power prediction. Renew. Energy, 221, 15, 119700. DOI: 10.1016/j.renene.2023.119700

He, X., Huang, J., Montillet, J.P., Wang, S., Kermarrec, G., Shum, C.K., ... Wang, F.: 2025, A noise reduction aproach for improve North American regional sea level change from satellite and in situ observations. Surv. Geophys., 1–32. DOI: 10.1007/s10712-025-09894-8

He, X., Montillet, J.P., Fernandes, R. et al.: 2022, Sea level rise estimation on the Pacific coast from southern California to Vancouver Island. Remote Sens., 14, 17, 4339. DOI: 10.3390/rs14174339

He, X., Montillet, J.P., Kermarrec, G. et al.: 2024, Space and Earth observations to quantify present-day sea-level change. Adv. Geophys., 65, 1, 125–177. DOI: 10.1016/bs.agph.2024.06.001

Ishida, K. et al.: 2020, Hourly-scale coastal sea level modeling in a changing climate using long short-term memory neural network. Sci. Total Environ., 720, 137613. DOI: 10.1016/j.scitotenv.2020.137613

Jean-Michel, L., Eric, G., Romain, B.B. et al.: 2021, The Copernicus global 1/12 oceanic and sea ice GLORYS12 reanalysis. Front. Earth Sci., 9, 698876. DOI: 10.3389/feart.2021.698876

Jiao, J., Wang, H., Dang, Y., Ren, Y., Yue, C., Wu, X., ...,Wang, X.: 2025, Noise-resilient GNSS coordinate time series prediction using AVMD-sLSTM-transformer hybrid model. Adv. Space Res., 76, 11. DOI: 10.1016/j.asr.2025.09.04

Jin, T., Xiao, M., Jiang, W. et al.: 2021, An adaptive method for nonlinear sea level trend estimation by combining EMD and SSA. Earth Space Sci., 8, 3, e2020EA001300. DOI: 10.1029/2020EA001300

Khan, A., Rauf, Z., Sohail, A., Khan, A.R., Asif, H., Asif, A. and Farooq, U.: 2023, A survey of the vision transformers and their CNN-transformer based variants. Artif. Intell. Rev., 56 (Suppl 3), 2917–2970. DOI: 10.1007/s10462-023-10595-0

LeCun, Y., Bottou, L., Bengio, Y. and Haffner, P.: 1998, Gradient-based learning applied to document recognition. Proc. IEEE, 86, 11, 2278–2324. DOI: 10.1109/5.726791

Liu, J., Jin, B., Wang, L. et al.: 2020, Sea surface height prediction with deep learning based on attention mechanism. IEEE Geosci. Remote Sens. Lett., 19, 1–5. DOI: 10.1109/LGRS.2020.3039062

Londhe, S.N.: 2011, Forecasting water levels using artificial neural networks. Int. J. Ocean Clim. Syst., 2, 2, 119–135. DOI: 10.1260/1759-3131.2.2.119

Luo, H., Jiang, Y., Xu, Q. et al.: 2022, A spatio-temporal network for landslide displacement prediction based on deep learning. Acta Geod. Cartogr. Sin., 51, 2160.

Makarynskyy, O., Makarynska, D., Kuhn, M. et al.: 2004, Predicting sea level variations with artificial neural networks at Hillarys Boat Harbour, Western Australia. Estuar. Coast. Shelf Sci., 61, 2, 351–360. DOI: 10.1016/j.ecss.2004.06.004

Moore, J.C., Grinsted, A., Zwinger, T. and Jevrejeva, S.: 2013, Semiempirical and process-based global sea level projections. Rev. Geophys., 51, 3, 484–522. DOI: 10.1002/rog.20015

Mu, D., Ludwigsen, C.B., Peng, F., Yan, H. and Xu, T.: 2025a, Modeling sea level rise over 1993–2022: Implications for understanding coastal observations. Geophys. Res. Lett., 52, 20, e2025GL117434

Mu, D., Huang, R., Yin, P., Yan, H. and Xu, T.: 2025b, Reconstructing sea level rise at global 945 tide gauges since 1900. Earth Syst. Sci. Data Discuss., 1–30. DOI: 10.5194/essd-2025-300

Nicholls, R.J. and Cazenave, A.: 2010, Sea-level rise and its impact on coastal zones. Science, 328, 5985, 1517–1520. DOI: 10.1126/science.1185782

Nie, Q., Wan, D. and Wang, R.: 2021, CNN BiLSTM water level prediction method with attention mechanism. J. Phys. Conf. Ser., 2078. DOI: 10.3390/w16091227

Nidhinarangkoon, P., Ritphring, S. and Udo, K.: 2020, Impact of sea level rise on tourism carrying capacity in Thailand. J. Mar. Sci. Eng., 8, 2, 104. DOI: 10.3390/jmse8020104

Nieves, V., Radin, C. and Camps-Valls, G.: 2021, Predicting regional coastal sea level changes with machine learning. Sci. Rep., 11, 1. DOI: 10.1038/s41598-021-87460-z

Park, J.-Y., Schloesser, F., Timmermann, A. et al.: 2023, Future sea-level projections with a coupled atmosphere-ocean-ice-sheet model. Nat. Commun., 14, 1. DOI: 10.1038/s41467-023-36051-9

Pugh, D., Woodworth, P.L. and Woodworth, P.: 2014, Sea-level science: Understanding tides, surges, tsunamis and mean sea-level changes. Cambridge University Press. DOI: 10.1017/CBO9781139235778

Qi, H., Zhou, H., Dong, J. et al.: 2023, Small sample image segmentation by coupling convolutions and transformers. IEEE Transactions on Circuits and Systems for Video Technology, (TCSVT), 34, 7, 5282–5294. DOI: 10.1109/TCSVT.2023.3343632

Raj, N. and Brown, J.: 2023, Prediction of mean sea level with GNSS-VLM correction using a hybrid deep learning model in Australia. Remote Sens., 15, 11, 2881. DOI: 10.3390/rs15112881

Radebach, A., Donges, J.F., Donner, R.V., Barbosa, S., Lange, H. and Kurths, J.: 2013, Spatial patterns in nonlinear sea-level dynamics inferred from global satellite altimetry data. In: EGU General Assembly Conference Abstracts, EGU2013-8357.

Sorkhabi, O.M., Shadmanfar, B. and Al-Amidi, M.M.: 2023, Deep learning of sea-level variability and flood for coastal city resilience. City Environ. Interact., 17, 100098. DOI: 10.1016/j.cacint.2022.100098

Srivastava, P.K., Islam, T., Singh, S.K. et al.: 2016, Forecasting Arabian Sea level rise using exponential smoothing state space models and ARIMA from TOPEX and Jason satellite radar altimeter data. Meteorol. Appl., 23, 4, 633–639. DOI: 10.1002/met.1585

Steele, M. and Ermold, W.: 2007, Steric sea level change in the Northern Seas. J. Clim., 20, 3, 403–417. DOI: 10.1175/JCLI4022.1

Su, H., Li, X., Yang, B. and Wen, Z.: 2018, Wavelet support vector machine-based prediction model of dam deformation. Mech. Syst. Signal Process., 110, 412–427. DOI: 10.1016/j.ymssp.2018.03.022

Sun, X., Lu, T., Hu, S. et al.: 2024, A new algorithm for predicting dam deformation using grey wolf-optimized variational mode long short-term neural network. Remote Sens., 16, 21, 3978. DOI: 10.3390/rs16213978

Teja, K., Tiwari, R. and Mohanty, S.: 2020, Adaptive denoising of ECG using EMD, EEMD and CEEMDAN signal processing techniques. J. Phys. Conf. Ser., 1706, 1, 012077. DOI: 10.1088/1742-6596/1706/1/012077

Torres, M.E., Colominas, M.A., Schlotthauer, G. et al.: 2011, A complete ensemble empirical mode decomposition with adaptive noise. Proc. 2011 IEEE International Conference on Acoustics, Speech and Signal Processing (ICASSP), 4144–4147. DOI: 10.1109/ICASSP.2011.5947265

Uluocak, I.: 2025, Comparative study of multivariate hybrid neural networks for global sea level prediction through 2050. Environ. Earth Sci., 84, 3. DOI: 10.1007/s12665-025-12090-x

Vaswani, A. et al.: 2017, Attention is all you need. Adv. Neural Inf. Process. Syst., 30. DOI: 10.48550/arXiv.1706.03762

Wang, S., Shum, C.K., Bevis, M., He, X., Zhang, Y., Ding, Y., Zhang, C. and Montillet, J.P.: 2025, Sea level reconstruction reveals improved separations of regional climate and trend patterns over the last seven decades. Earth Syst. Sci. Data Discuss. DOI: 10.5194/essd-2025-251.

Wang, J., Tang, J. and Guo, K.: 2022, Green bond index prediction based on CEEMDAN-LSTM. Front. Energy Res., 9, 793413. DOI: 10.3389/fenrg.2021.793413

Yao, W., Bai, J., Liao, W., Chen, Y., Liu, M. and Xie, Y.: 2024, From CNN to transformer: A review of medical image segmentation models. J. Imaging Inform. Med., 37, 4, 1529–1547. DOI: 10.1007/s10278-024-00981-7

Yeh, J. R., Shieh, J. S. and Huang, N.E.: 2010, Complementary ensemble empirical mode decomposition: A novel noise enhanced data analysis method. Adv. Adapt. Data Anal., 2, 2, 135–156.

Yuan, J., Zhou, F., Guo, Z., Li, X. and Yu, H.: 2023, HCformer: hybrid CNN-transformer for LDCT image denoising. J. Digit. Imaging, 36, 5, 2290–2305. DOI: 10.1007/s10278-023-00842-9

Zhao, J., Cai, R. and Sun, W.: 2021, Regional sea level changes prediction integrated with singular spectrum analysis and long-short-term memory network. Adv. Space Res., 68, 11, 4534–4543. DOI: 10.1016/j.asr.2021.08.017

Zhou, Y., He, X., Montillet, J.P. et al.: 2025, An improved ICEEMDAN-MPA-GRU model for GNSS height time series prediction with weighted quality evaluation index. GPS Solut., 29, 3, 1–19. DOI: 10.1007/s10291-025-01867-z

Zubier, K.M. and Eyouni, L.S.: 2020, Investigating the role of atmospheric variables on sea level variations in the Eastern Central Red Sea using an artificial neural network approach. Oceanologia, 62, 3, 267–290. DOI: 10.1016/j.oceano.2020.02.002